doi.org/10.52866/esj.2026.09.27.21

Experimental determination of the radiation dose rate in a materials equivalent to bone tissue

Mohsin Hasan Ali
Department of Physics, College of Education for Pure Science,
University of Tikrit, Tikrit, Iraq.
E-mail:muhsin.astro@tu.edu.iq

Abstract :

This study aimed to produce bone-like materials by investigating the radiation dose rate and mass attenuation coefficients (MACs) of eight metal-organic epoxy samples reinforced with different amounts of sodium chloride (NaCl). Gamma rays with an intensity of 60, 186, 242, 295, 352, 609, and 662 keV were used. These rays came from nuclear sources emitting ^{241}Am, ^{226}Ra, and ^{137}Cs isotopes. A NaI(Tl) gamma ray detector was used to perform the measurements. The results showed that increasing the amount of the (NaCl) activator slowed the radiation dose rate. On the other hand, increasing the power and efficiency of the source significantly increased the dose rate. With a difference of less than 3%, the observed (MAC) values were very close to the figures reported in ICRU Report No. 44. The results demonstrate that the manufactured composite materials can be used in place of conventional materials for dosimetry tasks, and can also be used in place of conventional materials to make tissue phantoms for medical and imaging studies.

Keywords: Radiation dose, Attenuation coefficients, γ- γ-radiation, NaI(Tl) detector, Exposure rate.

التحديد التجريبي لمعدل جرعة الإشعاع في مواد مكافئة لأنسجة العظام

محسن حسن علي
قسم الفيزياء ، كلية التربية للعلوم الصرفة، جامعة تكريت ، تكريت ، العراق.
البريد الالكتروني: muhsin.astro@tu.edu.iq

مستخلص:

في هذه الدراسة، حُدد معدل جرعة الإشعاع ومعاملات التوهين الكتلي لثماني عينات مُحضرة من مركب عضوي (إيبوكسي) مدعم بنسب وزنية مختلفة من كلوريد الصوديوم (NaCl)، بهدف تطوير مواد مُكافئة لأنسجة العظام. استُخدمت طاقات أشعة كاما 60، 186، 242، 295، 352، 609، و662 كيلو إلكترون فولت، مُنبعثة من مصادر مشعة من ^{241}Am و^{226}Ra و^{137}Cs، وأُجريت القياسات باستخدام مطياف أشعة غاما NaI (Tl). أشارت النتائج إلى أن زيادة تركيز كلوريد الصوديوم المدعم أدى إلى انخفاض معدل جرعة الإشعاع، بينما أدى ارتفاع طاقة المصدر وكفاءته إلى زيادة معدل الجرعة. كانت معاملات التوهين الكتلي المُقاسة مُتوافقة تمامًا مع القيم الواردة في تقرير ICRU-44 ، بانحراف أقل من ٪3. وتؤكد هذه النتائج أن المواد المركبة المحضرة تعد مرشحة واعدة لتطبيقات قياس الجرعات ويمكن أن تكون بمثابة مواد بديلة لتصنيع مجسمات الأنسجة في الأبحاث الطبية والإشعاعية.

الكلمات المفتاحية: جرعة الاشعاع، معاملات التوهين، إشعاع كاما ، كاشف ايوديد الصوديوم ، معدل التعرض.

1. Introduction

For radiation dosimetry and calibration in medical imaging, it is important to study the tissue-equivalent materials used to create models. These materials consist of several chemicals that work together in a manner similar to how human flesh reacts to atomic radiation. The manufactured material must have absorption properties as close as possible to those of tissues that have been similarly irradiated. To create tissue-equivalent materials, it is crucial to know the physical properties of these materials and how they interact with radiation. Currently, various types of materials are used to create fake human organs and cells so that the harmful radiation exposure to patients can be measured. Tissue-equivalent materials are the name for these types of materials. They are widely used in medical physics, such as therapeutic radiology, nuclear medicine, and diagnostic imaging [1-5].

For dosimetry studies, tissue-equivalent materials are often used to look like human tissue. People exposed to ionizing radiation can obtain accurate estimates of their radiation doses from these materials, which can also be used as substitutes for real living cells in radiation studies. Radiation attenuation in a material is determined by things like linear and mass attenuation coefficients, which describe how likely photons are to interact with the material per unit length or mass. These are extremely important in fields such as radiography, dosimetry, and medical imaging [6-11].

These things are extremely important. To prevent healthy organs from being overexposed to radiation, it is important to fully understand how cells in radiotherapy reduce radiation exposure. Radiation overexposure can be reduced by using appropriate radiation sources and correctly identifying tissue type and thickness [12-17]. Getting the right attenuation coefficients is important for better treatment plans, creating phantoms, and making medical and industrial uses safer [18-20].

This study aimed to investigate how to make bone-like products from sodium chloride (NaCl)-reinforced epoxy resins. We used a NaI(Tl) detector to verify the radiation dose rate and mass absorption coefficients of samples fabricated at gamma ray energies between 60 and 662 keV. The test results were then compared with those reported in ICRU Report No. 44 to determine the potential of these materials as bone-like substitutes.

2. Theoretical

2.1Activity of radionuclides

Radionuclide activity is a measure of the intensity of radiation emitted during radioactive decay, and is defined in the following equation [21, 22]:

$$A_i = -dN_i / dt = \lambda_i N_i \cdots (1)$$

Where A_i is the activity of a radioactive source isotope, equal to the number of radioactive decay nuclei dN_i at a given instant (dt) and proportional to the number of radioactive nuclei N_i at instant (t), and λ_i is the decay constant. The half-life ($t_{1/2}$) associated with the decay constant is given by the following relationship [23]:

$$t_{1/2} = \ln 2 / \lambda_i \cdots (2)$$

And the solution to the equation (1) is given as follows [24]:

$$N_i = N_0 e^{-\lambda t} \cdots (3)$$

Where N_0 is the number of nuclei at instant (t=0) and N_i is the number of nuclei at instant (t). The above equation can be written in terms of radioactivity as follows [24]:

$$A_i = A_0 e^{-\lambda t} \cdots (4)$$

Where A_0 is initial nucleus activity in time (t=0) and is final nucleus activity at time (t). The minus sign indicates the fact that radioactivity decreases with time.

2.2Radiation Dose

When ionizing radiation penetrates a substance, such as the human body, it deposits energy with it. Absorbed energy each unit mass of radiation exposure is called a dose. And the concept of dose may mean (dose absorbed, equivalent dose, equivalent effective dose). The radioactive forcing occurs only when transmitted energy from radiation to some material being irradiated, and possibly the radioactive effect is different when a certain amount of energy is added to a small mass of matter instead of distributing energy over a large mass. The change in energy absorbed (ΔE) per unit mass (m) called the absorbed radiation dose is measured in (Gray) units, as in the following equation [25]:

$$D = \Delta E / m \cdots (5)$$

As for the dose-rate, it represents the radiation dose per unit time ($Gray/hr$).

As in a given material medium, each photon in the beam is either completely removed from the beam by scattering or absorption, and this leads to an exponential weakening of the beam proportional to the thickness of the absorbing medium to the package or not interacting with the physical medium at all. The attenuation of a beam of gamma rays may be the attenuation of its energy or the attenuation of its intensity along the path through the medium [26]. The dose rate for a symmetric point radioactive source is given by the following relationship [27]:

$$D' = De^{-\mu x} \cdots (6)$$

$$D = \Gamma A_i / d^2 \cdots (7)$$

Where the fixed dose rate and (d) the distance between radiating source and the detector, where the factor ($\frac{\Gamma A_i}{d^2}$) is called exposure rate.

Since the rate of radiation dose in units ($\mu Sv/hr$) can be calculated using the following relationship [28]:

$$D = 0.142 \times A_i/d^2 \times \sum_i f \times E_\gamma \ldots (8)$$

Where (f) is ratio of number of gamma-ray emitted with a specific energy of line per (100) decay of the decay of the radioactive isotope and E_γ the energy of incident gamma ray.

When calculating the total radiation dose rate ($D't$) for a radioactive source that contains more than Energy we use the following relationship [28]:

$$D'_t = \sum_i D' \ldots (9)$$

2.3Attenuation of Radiation

The (μ_m) represents the rate of photon interactions within one mass unit per area unit (cm^2/g), which is given by the following equation [29]:

$$\frac{\mu_m}{\rho} = \frac{\ln\left(\frac{I_o}{I}\right)}{\rho x} \ldots (10)$$

where ρ represents the material's density.

3. Materials and Methods

3.1Samples Preparation

Epoxy resin (Sikadur-52 LP) and sodium chloride (NaCl) were used to prepare eight different mixtures with NaCl concentrations of 0, 2, 4, 6, 8, 10, 12, and 14 wt%. The epoxy components were mixed in a 2:1 ratio (base to hardener), after which NaCl was added in the desired proportions. The mixtures were poured into circular molds with a radius of 2.9 cm and a thickness of 0.5 cm, producing eight samples (labeled A–H). These samples were designed to simulate bone tissue by approximating fundamental atomic and physical properties such as electron density and molecular cross-section (Fig. 1a).

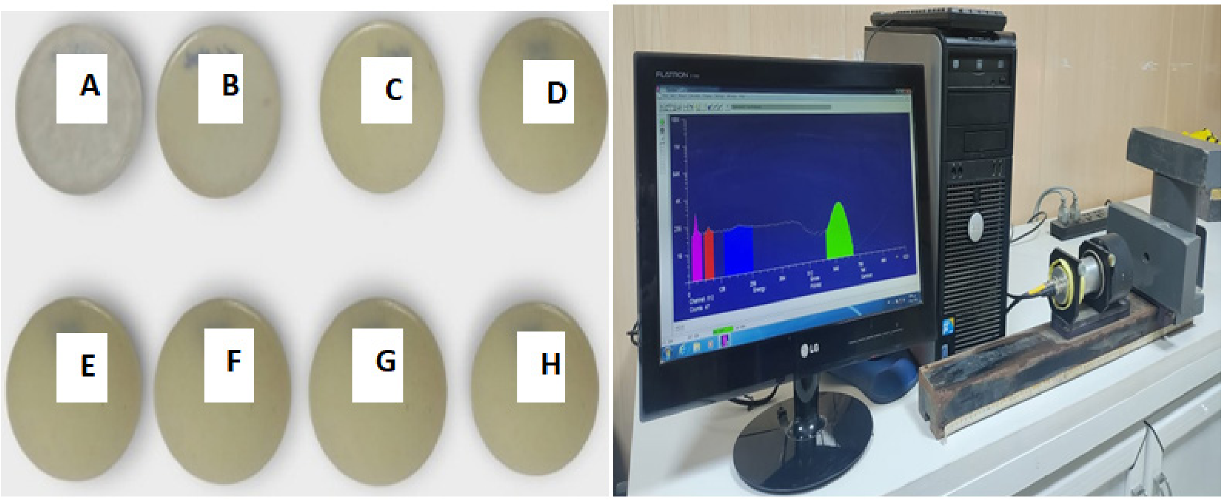

(a) (b)

Figure 1. (a) Some samples preparation A to H, (b) Set up experimental.

3.2Experimental Setup and Measurements

Experimental measurements were performed using a computer-based gamma-ray spectrometer system connected to a thallium-doped sodium iodide (NaI(Tl)) detector. The system included a preamplifier, a main amplifier, and a multichannel analyzer. A lead collimator (20 × 10 × 5 cm³) with a 15 mm aperture was used to obtain a narrow and well-defined gamma-ray beam (Fig. 1b).

Three sealed radioactive sources were used: ^{241}Am (60 keV, 74 kBq, half-life = 432 y), ^{137}Cs (662 keV, 400 kBq, half-life = 30.17 y), and ^{226}Ra (186–609 keV, 2 kBq, half-life = 1600 y). The samples were placed at a fixed distance of 15 cm from the detector, and the gamma-ray spectra were recorded for 900 s using USX PCI spectroscopy software. Measurements were repeated three times for each sample to improve statistical accuracy.

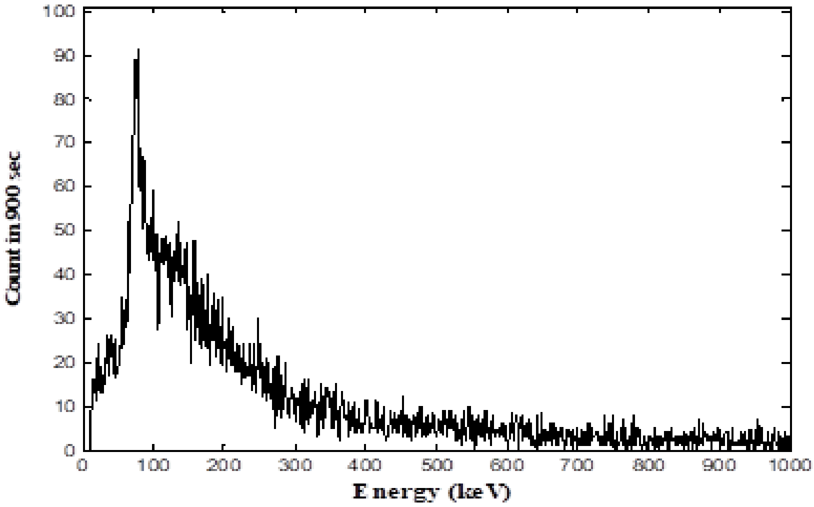

Figure 2. Background spectrum.

The gamma-ray attenuation of the prepared samples was analyzed using the Beer-Lambert law [29]. The mass attenuation coefficient (µm) was calculated from the ratio of the incident photon intensity to the transmitted photon intensity, with the absorber thickness fixed at 0.5 cm.

The radiation dose rate (µSv/h) was calculated using standard dosimetric equations that relate the activity of the source, photon emission probability, and gamma-ray energy [25–28]. For each sample, the dose rate was determined at different energies, and the results were compared with reference values reported in ICRU Report 44 [31], Figures (3-5).

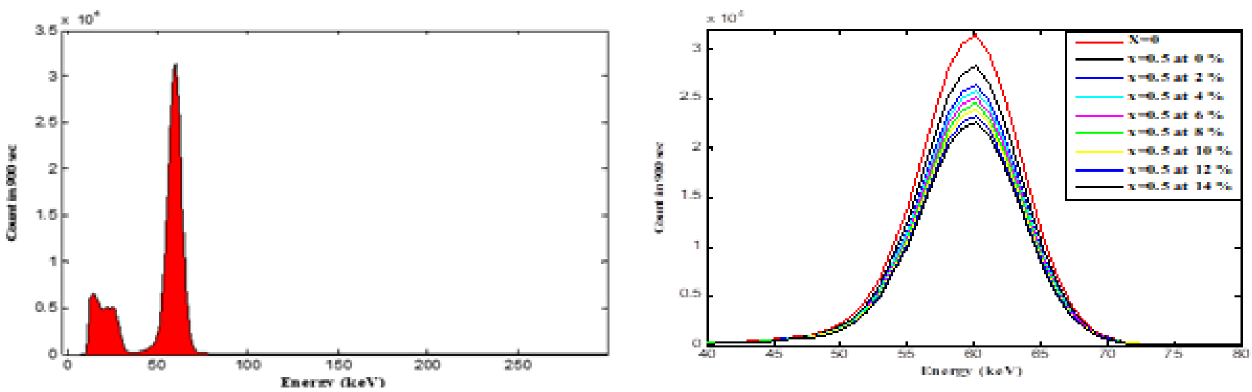

(a) (b)

Figure 3. The spectrum obtained for γ-ray spectroscopy for
(a) ^{241}Am (without samples). (b) . ^{241}Am (with samples).

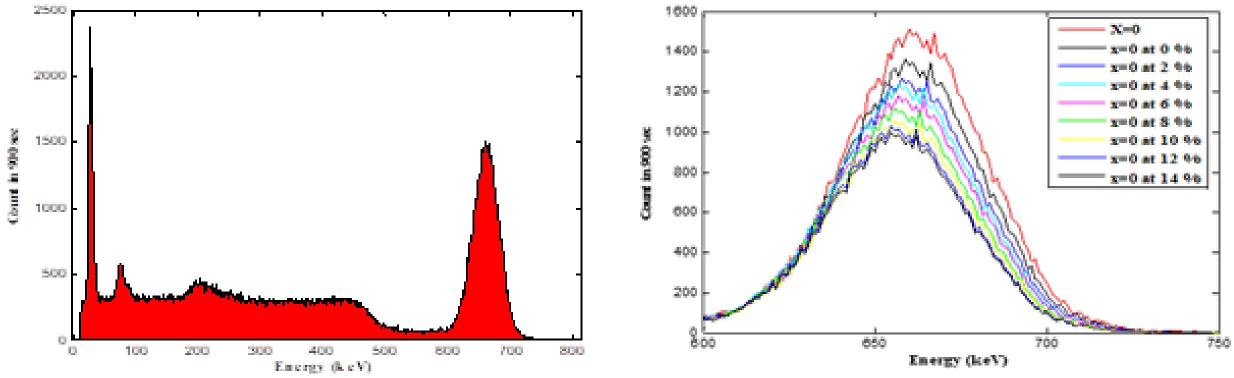

(a) (b)

Figure 4. The spectrum obtained for γ-ray spectroscopy for (a) ^{137}Cs (without samples). (b) . ^{137}Cs (with samples).

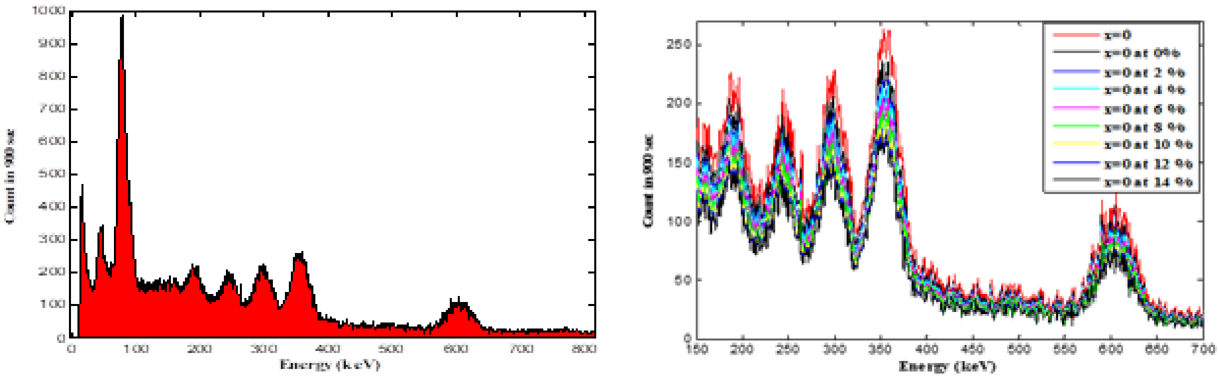

(a) (b)

Figure 5. for γ-ray spectroscopy for (a) ^{226}Ra (without samples). (b) . ^{226}Ra (with samples).

4.Results and discussion

The radiation dose rates for the prepared samples were calculated using Equation (6), and the results are summarized in Table 1. For samples of equal thickness, the radiation dose rate was found to decrease with increasing NaCl concentration. This reduction can be attributed to enhanced photon attenuation due to the higher density of the composites as more reinforcing material was added. Conversely, the dose rate increased with increasing gamma-ray energy, reflecting the higher photon flux and energy deposition associated with more energetic sources.

Table 1. radiation dose rate ($\mu Sv/hr$) of sample.

Sample	E(keV)						
	59.5	186	242	295	352	609	662
A	4.2068	5.4223	7.0828	8.6678	10.385	18.09	64.616
B	4.1617	5.3982	7.0521	8.6359	10.351	18.042	64.435
C	4.1134	5.3681	7.0214	8.6007	10.312	17.957	64.239
D	4.062	5.344	6.9908	8.5623	10.27	17.927	64.029
E	4.0119	5.3139	6.954	8.5272	10.232	17.867	63.822
F	3.9612	5.2899	6.9233	8.4888	10.188	17.806	63.611
G	3.9073	5.2598	6.8865	8.4472	10.145	17.74	63.385
H	3.8551	5.2297	6.8497	8.4089	10.101	17.679	63.163

The variation of the mass attenuation coefficient (μ_m) with NaCl concentration is presented in Figure 6a. The results demonstrate a clear trend of increasing (μ_m) with higher reinforcement levels for all photon energies. This indicates that NaCl acts as an effective attenuating component, enhancing photon scattering and absorption. These findings confirm that epoxy alone is not suitable as a tissue-equivalent substitute; however, its combination with NaCl produces composites with properties that closely resemble bone tissue.

The dependence of (μ_m) on photon energy is illustrated in Figure 6b. As expected, (μ_m) decreases with increasing photon energy. This behavior reflects the dominance of different interaction mechanisms across the studied energy range. At low energies (≤ 100 keV), the photoelectric effect dominates, leading to higher attenuation. In the intermediate energy region, Compton scattering is the primary interaction, resulting in a gradual decline in (μ_m). At higher energies (> 500 keV), pair production becomes more significant, and (μ_m) tends to stabilize.

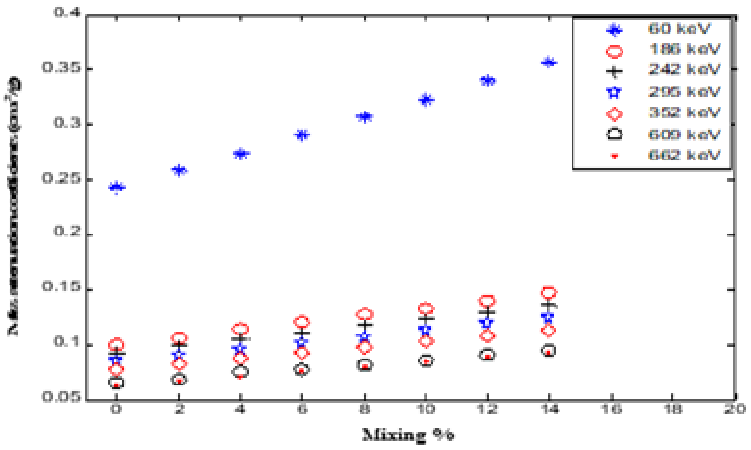

(a)

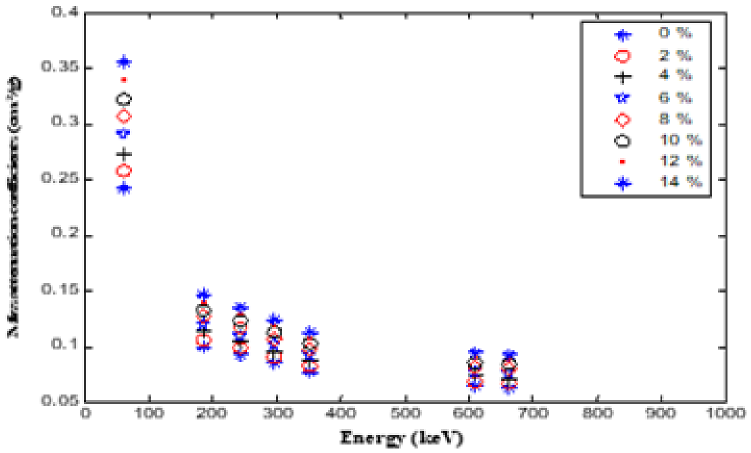

(b)

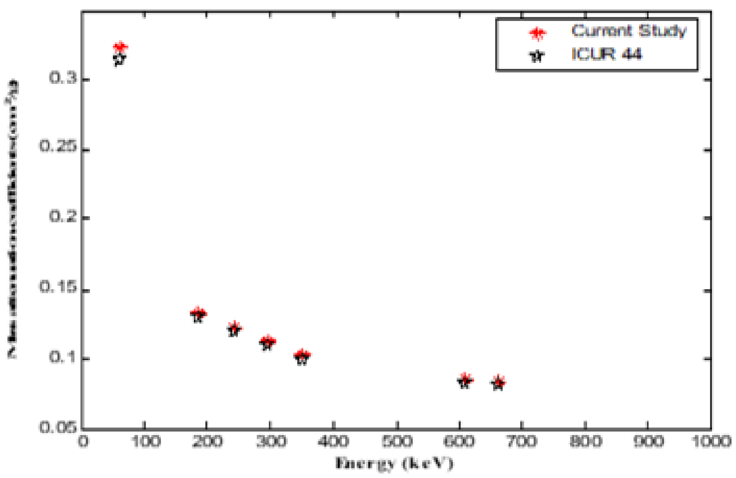

(c)

Figure 6. μ_m with
(a) wt%, (b) Energy, (c) comparative of mass attenuation coefficients.

The micrometer test values for the specimen that achieved the best result (E) are shown in Figure 6c, next to the reference values from ICRU Report No. 44. With differences of less than 3%, the two data sets are very close. This accuracy demonstrates that the experiment was performed correctly and proves that the composites were fabricated to be tissue-equivalent.

Overall, the results demonstrate that the fabricated epoxy-sodium chloride composites successfully mimic the resorption properties of bone tissue. By carefully varying the sodium chloride content, the density and resorption properties of the material can be made to closely match those of living tissue. Such materials are valuable in dosimetric studies, radiation shielding, and the fabrication of phantoms for medical imaging and radiotherapy applications.

5. Conclusion

This work investigated the radiation dose rate and mass absorption coefficients of resin and sodium chloride mixtures with different amounts of sodium chloride. The results showed that the radiation dose rate decreased with increasing sodium chloride concentration, while the dose increased with increasing photon energy. Between 60 and 662 keV, the mass absorption values found were very close to those reported in ICRU Report 44, with a difference of only 3%.

The characteristic composition (E) was the most similar to the natural values for all samples studied. This means it could be used as a solid, bone-like material. The results demonstrate that sodium chloride-reinforced plastic could be used instead of real flesh in tests to determine the amount of radiation a person is exposed to, to examine radiation protection, and to create phantoms for nuclear medicine and therapeutics.

The results of this study demonstrate that composition, density, and photon energy all play a significant role in how radiation exchanges are slowed. By varying the number of supporting parts used, hybrid materials can be created with properties very similar to human flesh. This could improve the accuracy and safety of medical and research tasks that require harmful radiation.

References

1. Jones, A. K., Hintenlang, D. E., & Bolch, W. E. (2003). Tissue-equivalent materials for construction of tomographic dosimetry phantoms in pediatric radiology. Medical Physics, 30(8), 2072–2081. https://doi.org/10.1118/1.1589487
2. Amini, I., Akhlaghi, P., & Sarbakhsh, P. (2018). Construction and verification of a physical chest phantom from suitable tissue equivalent materials for computed tomography examinations. Radiation Physics and Chemistry, 150, 51–57. https://doi.org/10.1016/j.radphyschem.2018.05.005
3. Amin, N. B., Abualroos, N. J., & Zainon, R. (2020). Fabrication of anthropomorphic thyroid-neck phantom for dosimetry study in nuclear medicine. Radiation Physics and Chemistry, 166, 108462. https://doi.org/10.1016/j.radphyschem.2019.108462
4. Chandramohan, D., Cao, P., Han, M., An, H., Sunderland, J. J., Kinahan, P. E., Laforest, R., Hope, T. A., & Larson, P. E. (2020). Bone material analogues for PET/MRI phantoms. Medical Physics, 47(5), 2161–2170. https://doi.org/10.1002/mp.14117
5. Singh, G., Gupta, M. K., Dhaliwal, A. S., & Kahlon, K. S. (2015). Measurement of attenuation coefficient, effective atomic number and electron density of oxides of lanthanides by using simplified ATM-method. Journal of Alloys and Compounds, 619, 356–360. https://doi.org/10.1016/j.jallcom.2014.08.254
6. Frimaio, A., Nascimento, B. C., Barrio, R. M. M., Campos, L. L., & Costa, P. R. (2019). X-ray spectrometry applied for determination of linear attenuation coefficient of tissue-equivalent materials. Radiation Physics and Chemistry, 160, 89–95. https://doi.org/10.1016/j.radphyschem.2019.02.012
7. Yastrebinskii, R. N. (2018). Attenuation of neutron and gamma radiation by a composite material based on modified titanium hydride with a varied boron content. Russian Physics Journal, 60, 2164–2168. https://doi.org/10.1007/s11182-018-1341-6

8. Jarrah, I., Radaideh, M. I., & Kozlowski, T. (2019). Determination and validation of photon energy absorption buildup factor in human tissues using Monte Carlo simulation. Radiation Physics and Chemistry, 160, 15–25. https://doi.org/10.1016/j.radphyschem.2019.02.002
9. Pavlenko, V. I., Cherkashina, N. I., Noskov, A. V., & others. (2016). Calculation of gamma photon propagation processes in a composite material. Russian Physics Journal, 59, 1192–1197. https://doi.org/10.1007/s11182-016-0890-9
10. Pavlenko, V. I., Yastrebinskii, R. N., & Lipkanskii, V. M. (2003). Simulation of the processes of gamma-radiation transport through shielding containers for radioactive waste. Russian Physics Journal, 46, 1062–1065. https://doi.org/10.1023/B:RUPJ.0000020821.53605.14
11. Kadri, O., & Alfuraih, A. (2019). Photon energy absorption and exposure buildup factors for deep penetration in human tissues. Nuclear Science and Techniques, 30(12), 176. https://doi.org/10.1007/s41365-019-0681-0
12. Coulaud, J., Brumas, V., Fiallo, M., Sharrock, P., Gonneau, E., Courbon, F., & Caselles, O. (2018). Tissue-inspired phantoms: A new range of equivalent tissue simulating breast, cortical bone and lung tissue. Biomedical Physics & Engineering Express, 4(3), 035017. https://doi.org/10.1088/2057-1976/aabb05
13. Apaza, G., Chen, F., & Vega, J. (2019). Construction and characterization of materials equivalent to the tissues and organs of the human body for radiotherapy. Radiation Physics and Chemistry, 159, 70–75. https://doi.org/10.1016/j.radphyschem.2019.02.004
14. White, D. R. (1993). The design and manufacture of anthropomorphic phantoms. Radiation Protection Dosimetry, 49(1–3), 359–369.
15. Rafiei, M. M., & Tavakoli-Anbaran, H. (2018). Calculation of the exposure buildup factors for x-ray photons with continuous energy spectrum using Monte Carlo code. Journal of Radiological Protection, 38(1), 207–218. https://doi.org/10.1088/1361-6498/aa9a13

16. Maeda, K., Matsumoto, M., & Taniguchi, A. (2005). Compton-scattering measurement of diagnostic x-ray spectrum using high-resolution Schottky CdTe detector. Medical Physics, 32(6), 1542–1547. https://doi.org/10.1118/1.1915015
17. Kurudirek, M., & Kurucu, Y. (2019). Estimation of energy absorption buildup factors of some human tissues at energies relevant to brachytherapy and external beam radiotherapy. International Journal of Radiation Biology, 95(12), 1685–1695. https://doi.org/10.1080/09553002.2019.1635958
18. Olarinoye, I. O. (2017). Photon buildup factors for some tissues and phantom materials for penetration depths up to 100 MFP.
19. Kadri, O., Manai, K., & Alfuraih, A. (2016). Monte Carlo study of the cardiac absorbed dose during X-ray examination of an adult patient. Radiation Protection Dosimetry, 171(4), 431–437. https://doi.org/10.1093/rpd/ncw060
20. Alsaif, N. A. M., et al. (2021). Calculating photon buildup factors in determining the γ-ray shielding effectiveness of some materials susceptible to be used for the conception of neutrons and γ-ray shielding. Journal of Materials Research and Technology. https://doi.org/10.1016/j.jmrt.2021.01.013
21. Seltzer, S. M., et al. (2011). Fundamental quantities and units for ionizing radiation. ICRU Journal.
22. Chanthima, N., et al. (2017). Development of BaO–ZnO–B2O3 glasses as a radiation shielding material. Radiation Physics and Chemistry. https://doi.org/10.1016/j.radphyschem.2017.02.020
23. Silverman, M. P. (2015). Search for non-standard radioactive decay based on distribution of activities. EPL (Europhysics Letters), 112(2), 22001. https://doi.org/10.1209/0295-5075/112/22001
24. Nsiah-Akoto, I., Fletcher, J. J., Oppon, O. C., & Andam, A. B. (2011). Indoor radon levels and the associated effective dose rate determination at Dome in the Greater Accra Region of Ghana. Research Journal of Environmental and Earth Sciences.
25. Tsoulfanidis, N., & Landsberger, S.

(2021). Measurement and detection of radiation (4th ed.). CRC Press.

26. Raheem, Z. J., & Saied, B. M. (2019, July). Interaction of heavy ions with brain tissue. In AIP Conference Proceedings (Vol. 2123, No. 1, p. 020050). AIP Publishing LLC.

27. Shousha, H. A., Rabie, N., & Hassan, G. M. (2011). Experimental investigation of commercially available lead composite aprons used for diagnostic X-rays. Radiation Effects and Defects in Solids, 166(11), 845–852. https://doi.org/10.1080/10420150.2011.608871

28. Bolus, N. E. (2001). Basic review of radiation biology and terminology. Journal of Nuclear Medicine Technology, 29(2), 67–73.

29. Chantler, C. T., Tran, C. Q., Barnea, Z., Paterson, D., Cookson, D. J., & Balaic, D. X. (2001). Measurement of the x-ray mass attenuation coefficient of copper using 8.85–20 keV synchrotron radiation. Physical Review A, 64(6), 062506. https://doi.org/10.1103/PhysRevA.64.062506

30. Amin, N. A. B., Zukhi, J., Kabir, N. A., & Zainon, R. (2017). Determination of effective atomic numbers from mass attenuation coefficients of tissue-equivalent materials in the energy range 60 keV–1.33 MeV. IOP Conference Series: Journal of Physics: Conference Series, 851, 012018. https://doi.org/10.1088/1742-6596/851/1/012018

31. International Commission on Radiation Units and Measurements (ICRU). (1989). ICRU Report 44. Bethesda, MD, USA.